Electronic Supplementary Material (ESI) for Nanoscale.

Supporting Information

Ultrahigh areal capacity and long cycle stability sodium metal anodes boosted by 3D printed sodiophilic MXene/rGO microlattice aerogel

Denghui Pan,[a] Haoyuan Yang,[a] Yueyue Liu,[a] Hui Wang,[a,b] Tingting Xu,[a] Dezhi Kong,[a] Jingjing Yao,[c] Yumeng Shi,[d] Xinjian Li,[a] Hui Ying Yang[c,*] and Ye Wang[a,c,*]

[a] Key Laboratory of Material Physics, Ministry of Education, School of Physics and Microelectronics, Zhengzhou University, Zhengzhou 450052, P. R. China. E-mail: wangye@zzu.edu.cn

[b] Center of Super-Diamond and Advanced Films (COSDAF) and Department of Chemistry, City University of Hong Kong, Hong Kong SAR, 999077, P. R. China

[c] Pillar of Engineering Product Development, Singapore University of Technology and Design, 8 Somapah Road, 487372, Singapore. E-mail: yanghuiying@sutd.edu.sg

[d] College of Electronics and Information Engineering, Shenzhen University, Shenzhen 518060, P. R. China

*Corresponding author

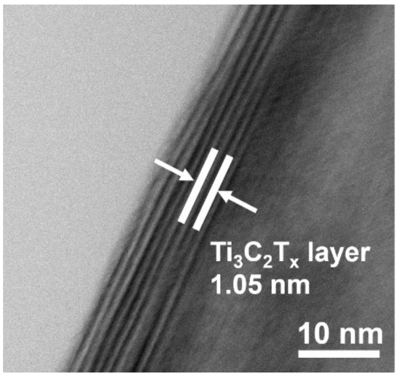

Fig. S1. TEM image of few-layer $Ti_3C_2T_x$.

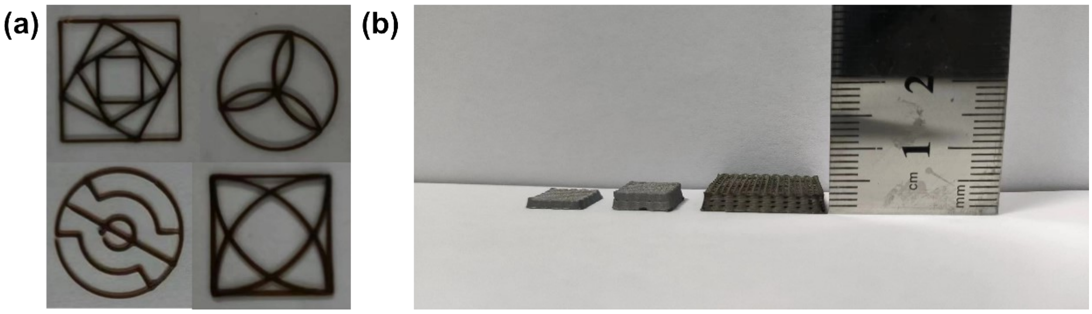

Fig. S2. Optical photos of $Ti_3C_2T_x$/rGO aerogels with (a) various patterns and (b) different layers (4, 8 layers) and different sizes (1×1, 2×2 cm) fabricated by the DIW 3D printing technique.

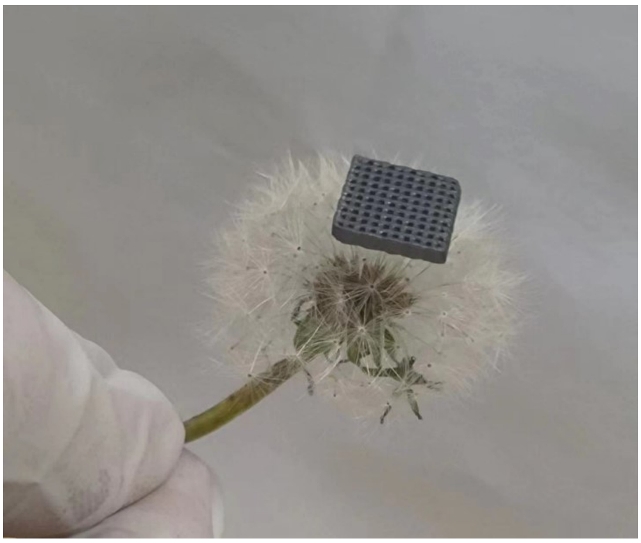

Fig. S3. An optical photograph of the 3D printed $Ti_3C_2T_x$/rGO aerogel on a dandelion to show the light weight.

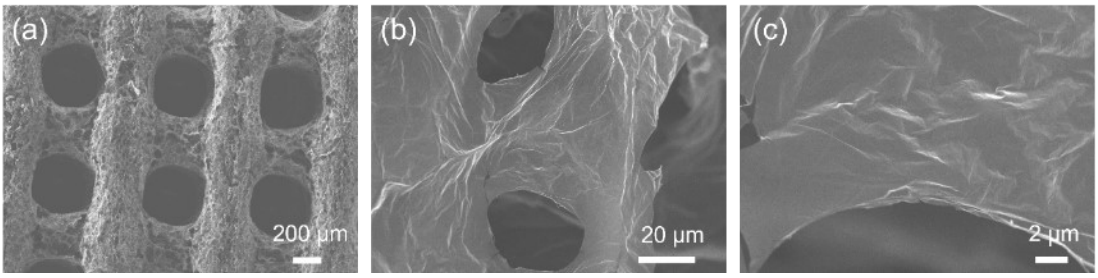

Fig. S4. SEM images of the 3D printed rGO aerogel electrodes.

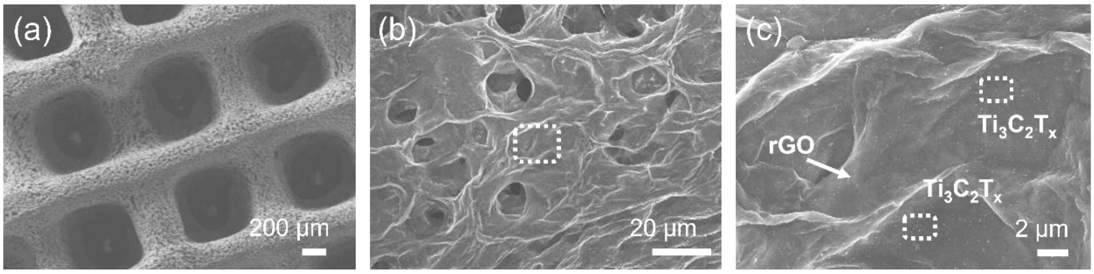

Fig. S5. SEM images of 3D printed 30% $Ti_3C_2T_x$/rGO aerogel electrodes.

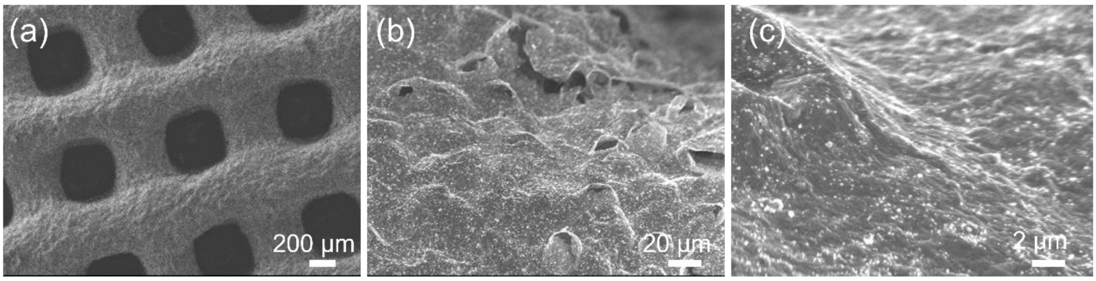

Fig. S6. SEM images of 3D printed 70% $Ti_3C_2T_x$/rGO aerogel electrodes

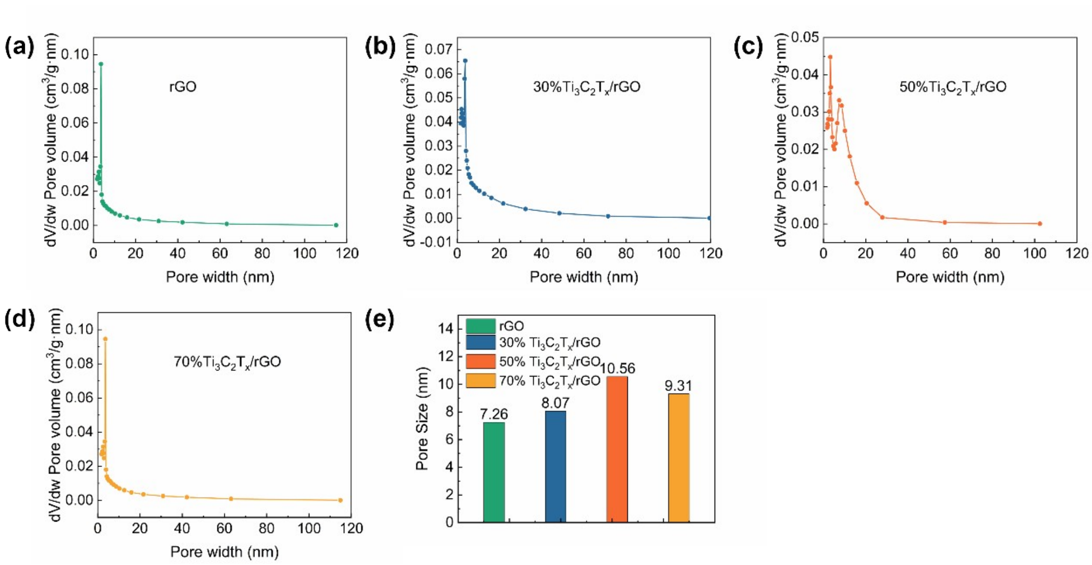

Fig. S7. BET pore-size distribution of 3D printed rGO, 30%, 50% and 70% $Ti_3C_2T_x$/rGO microlattice aerogel electrodes.

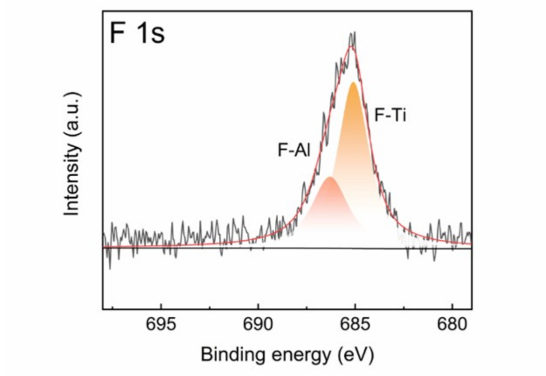

Fig. S8. XPS spectra of F 1s of $Ti_3C_2T_x$ nanocomposites.

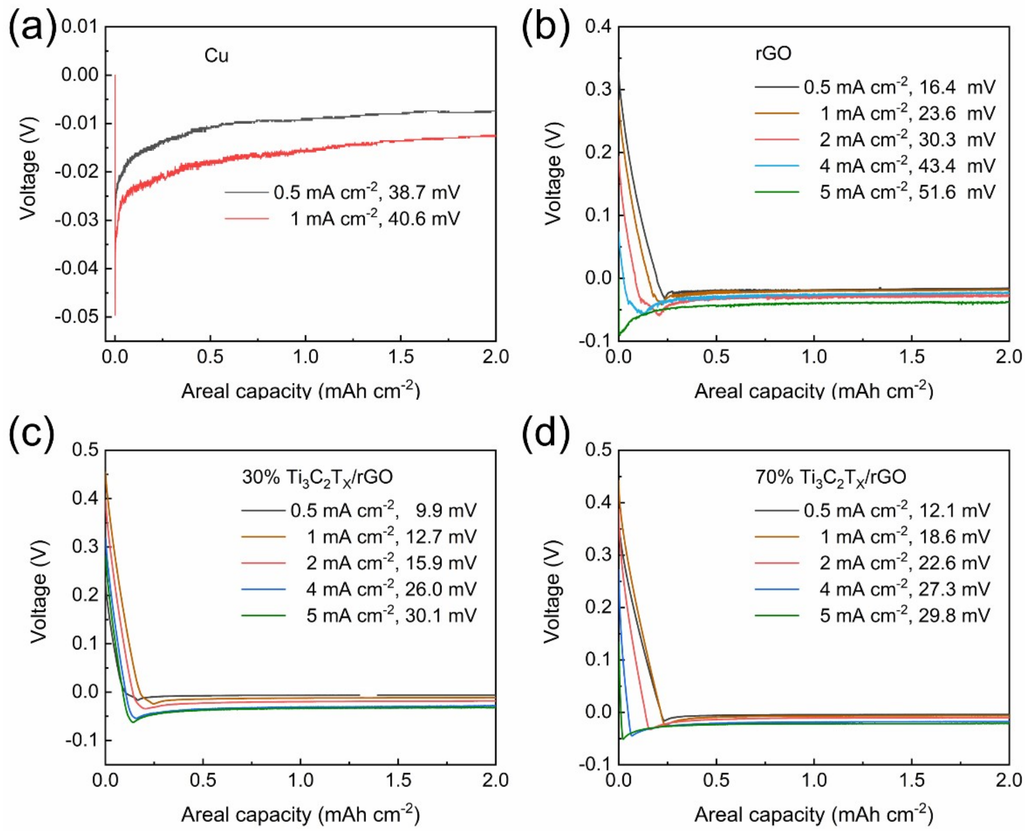

Fig. S9. Voltage-capacity curves of (a) Cu, 3D printed (b) rGO, (c) 30% $Ti_3C_2T_x$/rGO, (d) 70% $Ti_3C_2T_x$/rGO aerogel electrodes at different current densities.

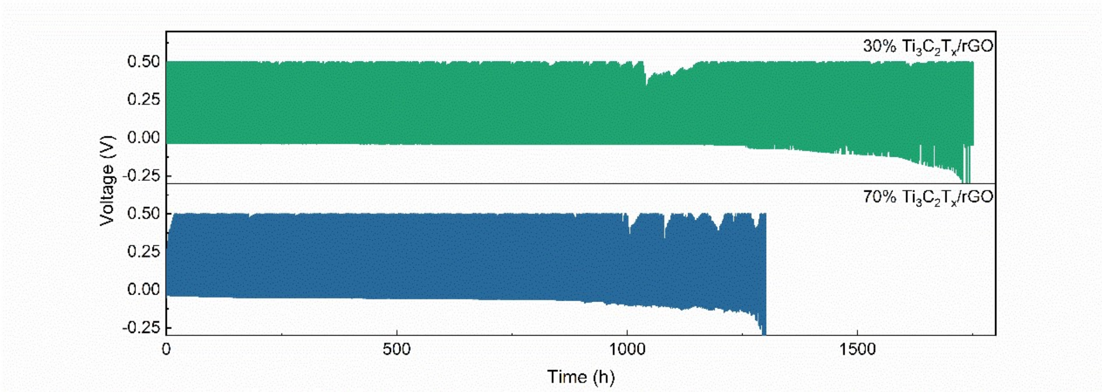

Fig. S10. Long cycle performance of 3D printed 30% $Ti_3C_2T_x$/rGO and 70% $Ti_3C_2T_x$/rGO electrodes at 2 mA cm^{-2} with 2 mAh cm^{-2}.

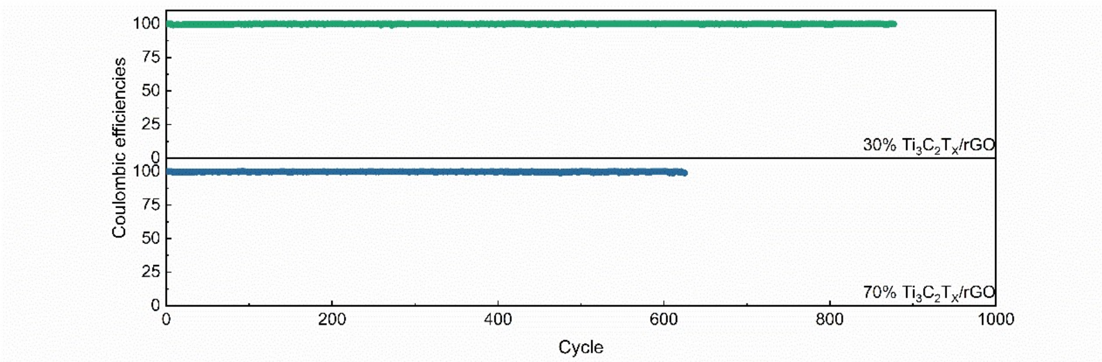

Fig. S11. CE of 3D printed 30% $Ti_3C_2T_x$/rGO and 70% $Ti_3C_2T_x$/rGO electrodes at 2 mA cm^{-2} with 2 mAh cm^{-2}.

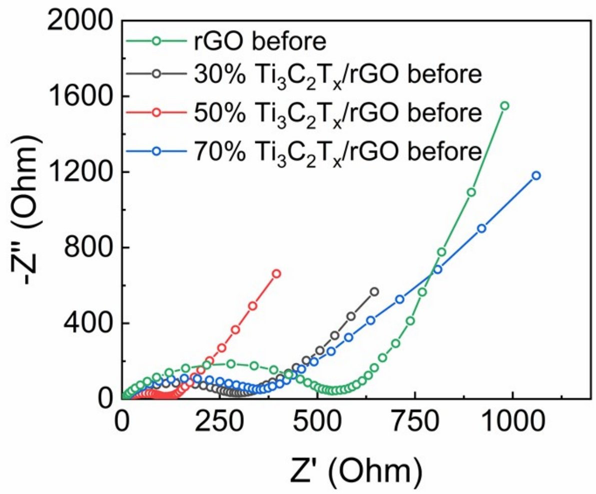

Fig. S12. EIS of the 3D printed rGO, 30%, 50%, 70% $Ti_3C_2T_x$/rGO aerogel electrodes before cycle at 2 mA cm^{-2} with 2 mAh cm^{-2}.

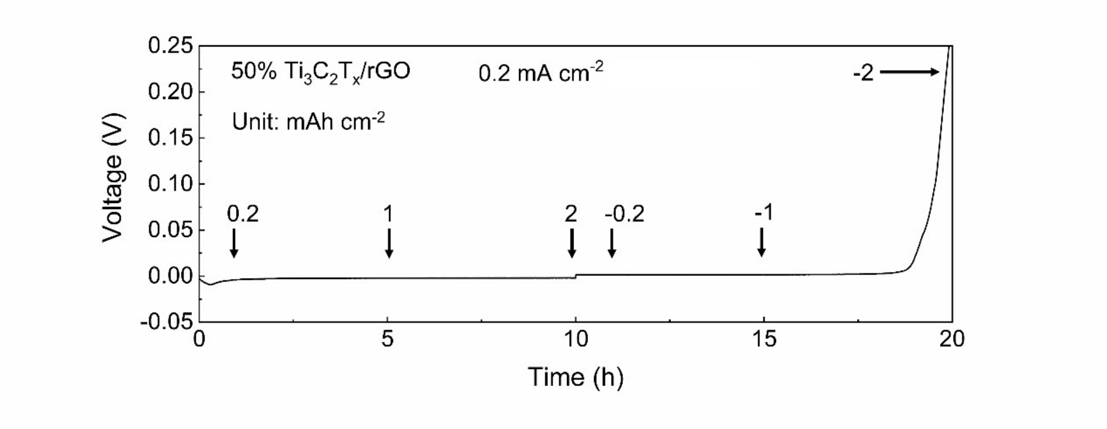

Fig. S13. The corresponding deposition-stripping curve for the morphological evolution of sodium deposition stripping on 3D printed 50% $Ti_3C_2T_x$/rGO electrodes.

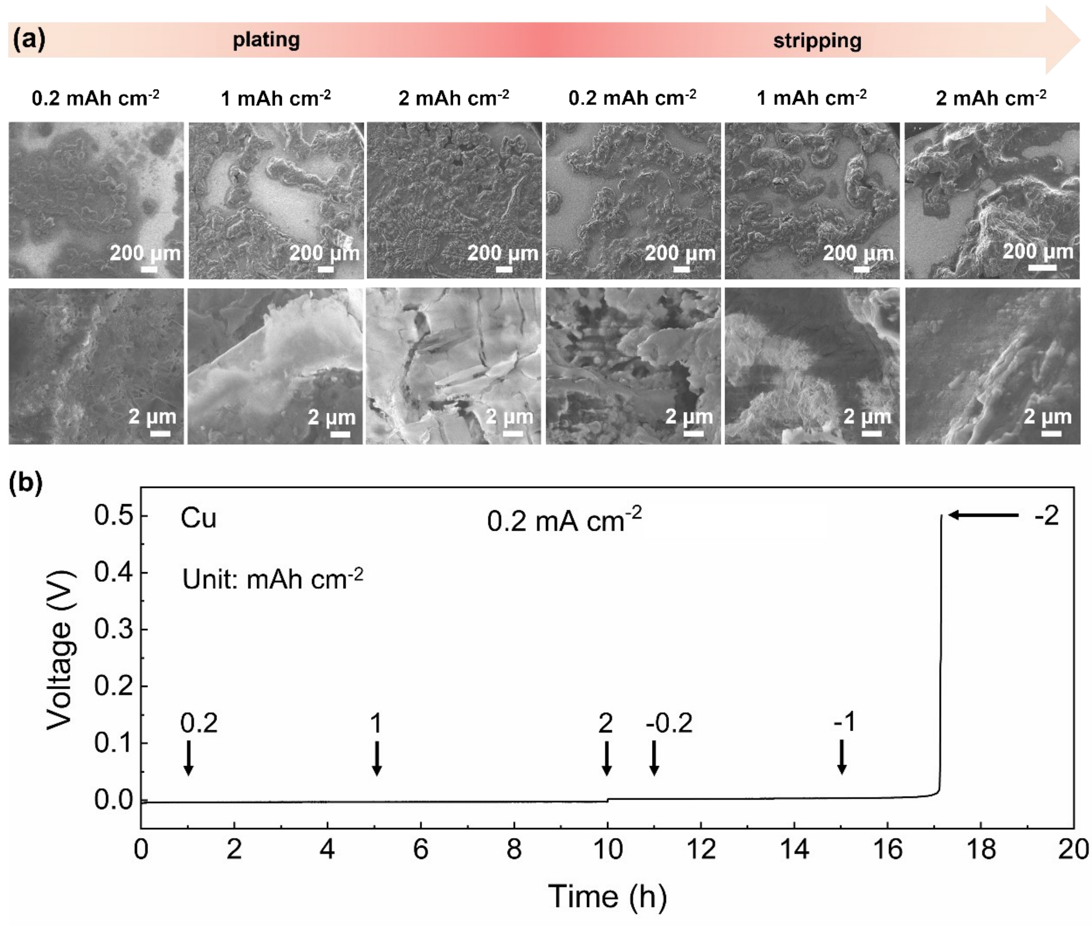

Fig. S14. (a) Morphology evolution of the sodium deposition and stripping on Cu electrode with the deposition capacities of 0.2, 1, 2 mAh cm^{-2}, stripping capacities of 0.2, 1, 2 mAh cm-

[2] (from left to right), and (b) corresponding deposition-stripping curve.

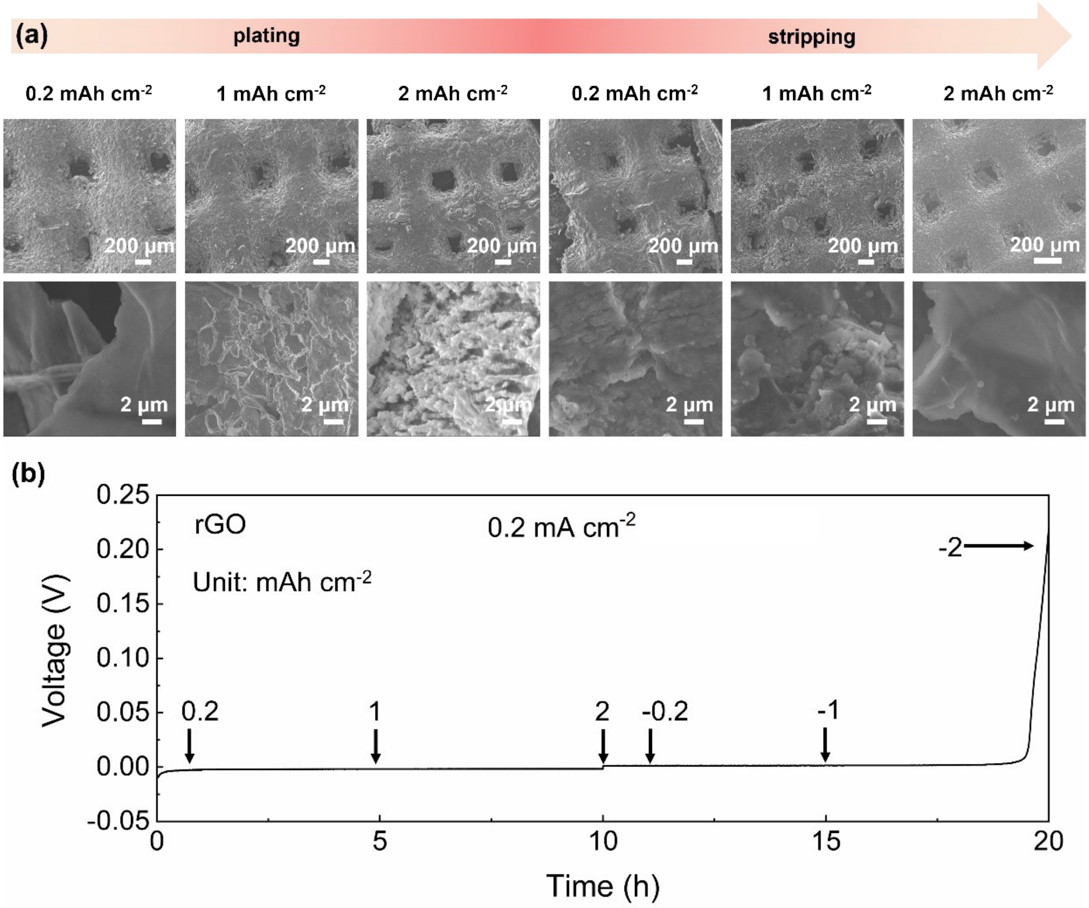

Fig. S15. Morphology evolution of the sodium deposition and stripping on 3D printed rGO electrode with the deposition capacities of 0.2, 1, 2 mAh cm^{-2}, stripping capacities of 0.2, 1, 2 mAh cm^{-2} (from left to right), and (b) corresponding deposition-stripping curve.

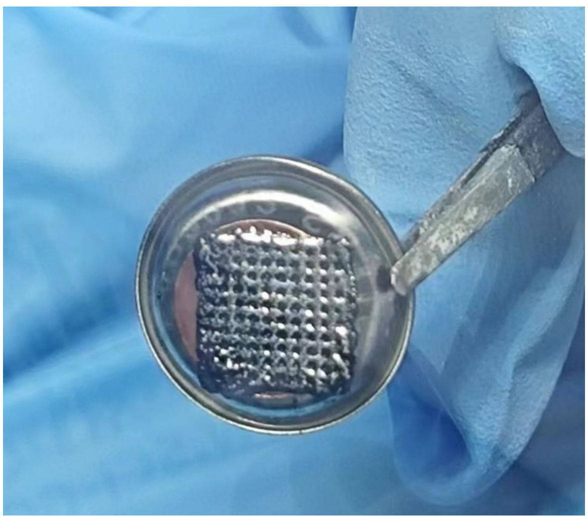

Fig. S16. Optical photographs of Na@$Ti_3C_2T_x$/rGO anode prepared by electrochemical deposition of 2 mAh cm^{-2} of Na.

Table S1. Exchange current density of the Cu, 3D printed rGO and 50% $Ti_3C_2T_x$/rGO electrodes.

Electrode	Exchange current density (mA cm^{-2})	Transfer coefficient
Cu	0.02	1.36
3D printed rGO	0.16	1.24
3D printed 50% $Ti_3C_2T_x$/rGO	5.01	1.30

Table S2. EIS fitting data of the 3D printed the rGO, 30%, 50%, 70% $Ti_3C_2T_x$/rGO microlattice electrodes.

Electrode	Before cycle R_{ct} (Ω)	After 30 cycles R_{ct} (Ω)	σ	D ($cm^2\ s^{-1}$)
3D printed rGO	546.89	62.53	12.34	6.44×10^{-15}
3D printed 30% $Ti_3C_2T_x$/rGO	353.57	25.49	9.09	1.19×10^{-14}
3D printed 50% $Ti_3C_2T_x$/rGO	112.17	16.21	8.61	1.32×10^{-14}
3D printed 70% $Ti_3C_2T_x$/rGO	299.15	40.23	9.27	1.14×10^{-14}

Table S3. Electrochemical performance comparison of various $Ti_3C_2T_x$ MXene-based Na metal anodes.

Electrode	Current density (mA cm^{-2})	Capacity (mAh cm^{-2})	Cycle time (h)	Cycle number	CE (%)	Reference
$Ti_3C_2T_x$-rGO Membrane	3	1	500	333		[1]
h-$Ti_3C_2T_x$/CNTs	1	1	4000	2000	99.2	[2]
Mg^{2+} Decorated $Ti_3C_2T_x$	0.5	0.5	200	100		[3]
$Ti_3C_2T_x$-CC	1	8	900	56	98.5	[4]
1D/2D $Na_3Ti_5O_{12}$-MXene	20	5	400	800	99.4	[5]
$Ti_3C_2T_x$@g-C_3N_4	1	1	700	350	99.9	[6]
3D printed 50% $Ti_3C_2T_x$/rGO	**2**	**2**	**3600**	**1800**	**99.91**	**This work**
3D printed 50% $Ti_3C_2T_x$/rGO	**5**	**50**	**1400**	**70**	**99.93**	**This work**

References

1. Y. Fang, Y. Zhang, K. Zhu, R. Lian, Y. Gao, J. Yin, K. Ye, K. Cheng, J. Yan, G. Wang, Y. Wei and D. Cao, *ACS Nano*, 2019, **13**, 14319-14328.
2. X. He, S. Jin, L. Miao, Y. Cai, Y. Hou, H. Li, K. Zhang, Z. Yan and J. Chen, *Angew.*

Chem. Int. Ed., 2020, **59**, 16705-16711.
3. H. Jiang, X. Lin, C. Wei, Y. Zhang, J. Feng and X. Tian, *Small*, 2022, **18**, 2107637.
4. Y. Fang, R. Lian, H. Li, Y. Zhang, Z. Gong, K. Zhu, K. Ye, J. Yan, G. Wang, Y. Gao, Y. Wei and D. Cao, *ACS Nano*, 2020, **14**, 8744-8753.
5. J. Luo, X. Lu, E. Matios, C. Wang, H. Wang, Y. Zhang, X. Hu and W. Li, *Nano Lett.*, 2020, **20**, 7700-7708.
6. C. Bao, J. Wang, B. Wang, J. Sun, L. He, Z. Pan, Y. Jiang, D. Wang, X. Liu, S. X. Dou and J. Wang, *ACS Nano*, 2022, **16**, 17197-17209.